Research Article | Vol. 9, No. 2 | 1 Feb 2019 | OPTICAL MATERIALS EXPRESS 643
Optical Materials EXPRESS

GLS and GLSSe ultrafast laser inscribed waveguides for mid-IR supercontinuum generation

MARK D. MACKENZIE,[1] JAMES M. MORRIS,[1,2] CHRISTIAN R. PETERSEN,[3] ANDREA RAVAGLI,[4] CHRIS CRAIG,[4] DANIEL W. HEWAK,[4] HENRY T. BOOKEY,[2] OLE BANG,[3] AND AJOY K. KAR[1,*]

[1]*Institute of Photonics and Quantum Sciences, David Brewster Building, Heriot-Watt University, Edinburgh, EH14 4AS, United Kingdom*
[2]*Fraunhofer Centre for Applied Photonics, Technology and Innovation Centre, 99 George Street, Glasgow G1 1RD, United Kingdom*
[3]*DTU Fotonik, Department of Photonics Engineering, Technical University of Denmark, DK-2800 Kgs. Lyngby, Denmark*
[4]*Optoelectronics Research Centre, University of Southampton, Salisbury Road, Southampton SO17 1BJ, United Kingdom*
**a.k.kar@hw.ac.uk*

Abstract: Using the ultrafast laser inscription technique, buried channel waveguides have been fabricated in gallium lanthanum sulfide and gallium lanthanum sulfide selenide glasses to demonstrate the suitability of the materials for supercontinuum generation in the mid-IR. Supercontinuum generation was performed using 100 femtosecond pump pulses with micro-Joule pulse energies and a center wavelength of 4.6 µm, which is in the anomalous dispersion regime for these waveguides. Under such pump conditions, supercontinuum was obtained covering a 25-dB-bandwidth of up to 6.1 um with a long-wavelength edge of 8 µm. To our knowledge, this represents the broadest and the longest-wavelength IR supercontinuum generated from an ultrafast laser inscribed waveguide to date.

1. Introduction

The development of chip-scaled photonic devices which operate in the near to mid-IR is of interest in a wide range of fields such as sensing, medicine and astronomy [1]. These applications also benefit from the scalability, robustness, and reduction in size that can be achieved when utilizing integrated optical systems over systems using free space optics. This requires the development of photonic light sources and devices compatible with the integrated optics approach and capable of operating in this wavelength region. Chalcogenide glasses are an important candidate as a host material for such devices as they have broad wavelength transmission across the mid-IR and high customizability in material composition, which allows for the tailoring of material properties and rare-earth doping [2–4].

Gallium lanthanum sulfide (GLS) and gallium lanthanum sulfide selenide (GLSSe) are two particularly promising chalcogenide glasses as they have excellent chemical and temperature resistance, broad wavelength transmission, high nonlinearity, and do not include some of the more toxic elements present in some other chalcogenides, such as arsenic (As) [5,6]. Making use of the high nonlinear response of GLS we have previously demonstrated supercontinuum generation (SCG) spanning 1.75-5 µm [7]. This compares well with similar results in other materials using waveguides fabricated by ultrafast laser inscription [8,9]. In this paper we show SCG in GLS channel waveguides near the limits of material transmission, achieved through improved waveguide optimization, characterization and optimized pump

#352021 https://doi.org/10.1364/OME.9.000643
Journal © 2019 Received 14 Nov 2018; revised 27 Dec 2018; accepted 27 Dec 2018; published 17 Jan 2019

Optical Materials EXPRESS

conditions. This then leads us to investigate GLSSe channel waveguides as a potential successor due to the improved transmission of GLSSe at infrared wavelengths, up to 15 μm, whilst otherwise retaining broadly similar properties to GLS [6].

For this study, buried channel waveguides were fabricated using ultrafast laser inscription (ULI). In ULI, femtosecond to few-picosecond pulses from an ultrafast laser are tightly focused inside a transparent dielectric material in order to modify its properties. Pulses are absorbed nonlinearly in the focal volume, generating high temperatures and pressures through an induced micro-plasma and leading to highly localized sub surface modification. This modification can include positive and negative refractive index change, used for forming waveguides [10]. Type I waveguides refers to those with a positive refractive index change where the light is guided in the modified regions, type II waveguides use the stress induced refractive index modification effect to guide between two modification regions and type III, depressed cladding waveguides, consists of an unmodified core surrounded by a number of negative refractive index change lines of modification. The benefits of ULI compared to other methods of fabricating waveguides such as lithography are its ability to rapidly prototype different designs, complete three-dimensional design freedom, no clean room requirement and its ability to modify a wide range of crystalline and amorphous materials [10–12].

SCG was demonstrated in the fabricated GLS channel waveguides covering a 25-dB-bandwidth of up to 6.1 um when pumped by 100 fs, 1.3 μJ pulses with 13 MW peak power at 4.6 um central wavelength. To our knowledge, this represents the broadest and longest-wavelength IR supercontinuum (SC) generated from a ULI fabricated waveguide to date and is comparable to supercontinuum generation in other types of chalcogenide based waveguides [13]. Similar broadening was found in channel GLSSe waveguides, covering a bandwidth of 5.8 μm for an input pulse energy of 1 μJ with 10 MW peak power. These results indicate the GLSSe is comparable to GLS as a host for channel waveguides for SCG.

2. Waveguide fabrication and characterization

Waveguides were fabricated in GLS (30% La_2S_3, 70% Ga_2S_3) and GLSSe (20% Ga_2Se_3, 30% La_2S_3, 50% Ga_2S_3) bulk samples using ULI, the relative transmission of these samples is shown in Fig. 1 as well as the transmission for GLSSe (60% Ga_2Se_3, 30% La_2S_3, 10% Ga_2S_3) showing the effect of increasing Se concentration. The transmission shown is for a sample of length 1 mm. For waveguide applications involving longer samples the usable IR transmission window will be decreased relative the maximum of 15 μm. The possible compositions of GLSSe and their material properties are discussed in detail by Ravagli et al [5,6]. The addition of Ga_2Se_3 to GLS increases its nonlinear refractive index, while for 20% level this effect is small it becomes more significant as the level increases. The inscription setup is shown in Fig. 2 and consists of a Yb-doped fiber laser (Amplitude Satsuma HP); optics for power and polarization control, beam shaping and focusing; and high precision positioning stages (Aerotech ABL1520 and ATS20030). Glass samples mounted on the translation stages are translated through the laser focus to create lines of modification and by making multiple parallel scans with a slight offset waveguides of arbitrary width can be fabricated, using a process referred to as the multiscan technique [14]. The waveguide height depends on the laser power and translation speed and can therefore be varied independently to the width.

Optical Materials EXPRESS

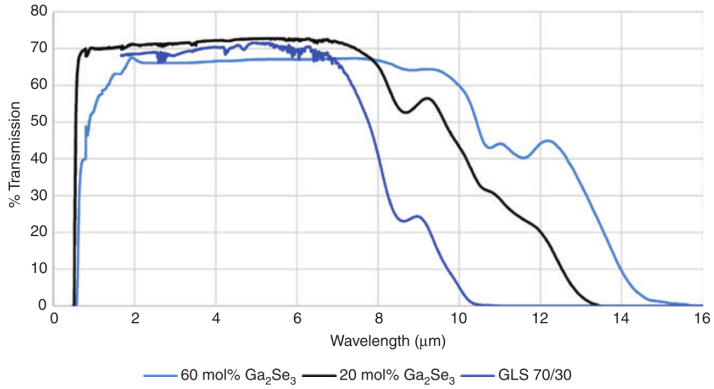

Fig. 1. Transmission spectrum of 1 mm thick GLS and GLSSe samples as given by Ravagli, A., et al. (2017) [6].

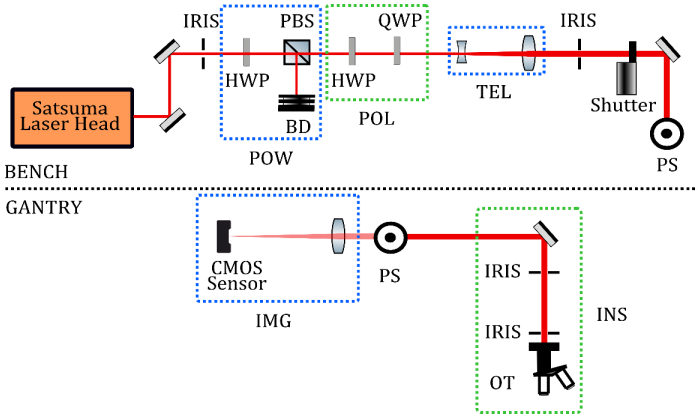

Fig. 2. Diagram of the ULI fabrication setup showing the inscription laser and optics for power control, POW; polarization control, POL; beam shaping, TEL; imaging, IMG; and beam delivery, INS. The translation stage, where samples are mounted, moves the samples through the focal region defined by the beam delivery optics for waveguide writing. HWP - half wave plate, PBS - polarising beam splitter, BD - beam dump, QWP - quarter wave plate, PS - periscope, OT – optics turret.

Waveguides were optimized through a parameter investigation to obtain low loss and single mode operation for a range of wavelengths in the near- to mid-IR. These parameters were then used to inscribe waveguides in two samples of GLS and GLSSe. In both materials, inscription was performed with a pulse repetition rate of 500 kHz, circular polarization and using a 0.4 NA aspheric lens for the final focusing of the inscribing beam into the samples. In order to fabricate multiscan waveguides an offset of 0.33 µm between parallel scans was utilized. For GLS, waveguides were inscribed with widths of 10 to 18 µm using writing speeds of 2 to 16 mm/s and pulse energies of 40 or 52 nJ. The sample length was 20 mm. This resulted in a range of waveguides with either rectangular or square cross section. Similar parameters were used for GLSSe. In this instance the sample length was 50 mm and waveguide widths of 4 to 20 µm were written using speeds of 2, 8 or 14 mm/s and pulse energies of 28, 36 and 44 nJ. This again resulted in a range of waveguides with square or rectangular cross section. The parameters for individual waveguides are given in Table 1 and from here onwards we will refer to individual waveguides as a material and number referring to this table, e.g. GLS-1. Samples were polished to enable efficient coupling of light to the waveguides. This variation and control of waveguide cross section is shown in Fig. 3(b)

Optical Materials EXPRESS

where it can be seen that for a given power and translation speed the height is fixed while an increasing number of scans increases the waveguide width.

Table 1. Inscription properties for waveguides used in SCG

Waveguide	Material	Width (µm)	Height (µm)	Pulse energy (nJ)	Speed (mm/s)	NA
GLS-1	GLS	18	19	52	2	0.4
GLS-2	GLS	14	19	52	2	0.4
GLSSe-1	GLSSe	20	22	44	2	0.4
GLSSe-2	GLSSe	16	22	44	2	0.4
GLSSe-3	GLSSe	12	22	44	2	0.4
GLSSe-4	GLSSe	8	22	44	2	0.4
GLSSe-5	GLSSe	4	22	44	2	0.4
GLSSe-6	GLSSe	20	17	36	2	0.4
GLSSe-7	GLSSe	16	17	36	2	0.4
GLSSe-8	GLSSe	12	17	36	2	0.4
GLSSe-9	GLSSe	8	17	36	2	0.4
GLSSe-10	GLSSe	4	17	36	2	0.4

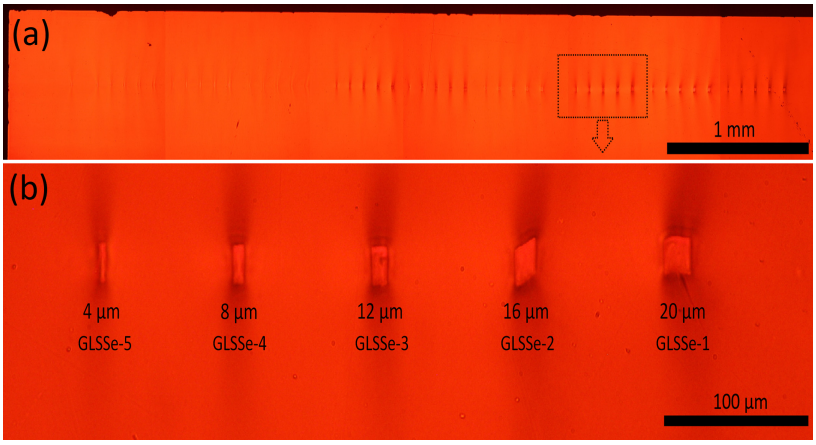

Fig. 3. Bright-field transmission microscopy images of waveguide end facets in GLSSe. (a) all waveguides with inscription power increasing from left to right. (b) subset showing size variation based on an increasing number of scans. In all instances the laser used for inscription was incident from top of image. The shape of GLSSe-2 is either due to an inscription error or non-uniform sample surface.

Waveguide loss measurements were taken using a continuous-wave HeNe laser operating at 3.39 µm. Coupling with 0.25 NA ZnSe objectives and measuring with a Thorlabs PDA20H-EC detector, the insertion loss was found to be 2.8 dB in GLS-2. For GLSSe-1 insertion loss was 2.4 dB. For comparison the absorption coefficient of pristine bulk GLS is 0.005 cm^{-1} and the reflection loss is 0.81 dB per surface. For a 20 mm long sample the total is then 1.71 dB.

3. Waveguide dispersion

Dispersion measurements were performed in bulk and waveguide samples using white light spectral-domain interferometry [15] with a mid-IR SC source (NKT Photonics), balanced Mach-Zehnder interferometer, and scanning spectrometer (Spectro 320 Instrument Systems). Results for similar ULI fabricated GLS waveguides have been presented previously by Demetriou *et al.* [16] and are summarized here for direct comparison with the GLSSe waveguides inscribed for this study, with waveguide parameters given in Table 2. In Fig. 4(a) bulk GLS dispersion is presented along with ULI fabricated buried channel waveguides inscribed using 64 nJ, 12 mm/s, 0.4 NA and 110 nJ, 12 mm/s, 0.6 NA, respectively. Both waveguides were fabricated using circular polarization and at a pulse repetition frequency of

Optical Materials EXPRESS

500 kHz. The waveguides show only a small change in dispersion compared to the bulk and the waveguides themselves are similar despite having different inscription parameters.

Figure 4(b) compares GLS channel waveguides of increasing size, but constant height (18 µm). Excluding Wg-1, all waveguides show similar zero-dispersion wavelength (ZDW), with the lower value for Wg-1 being attributed to its small size causing more of the guided light to interact with the bulk. These results show that the ZDW of bulk GLS is 3.61 µm with waveguides having slightly increased values between 3.66 and 3.71 µm. This increase in the waveguides is due to their low NA and large dimensions, similar effects have been seen fibers [17]. While waveguide inscription parameters have an impact of dispersion this is a weak effect compared to the effect of inscription parameters have on waveguide transmission and MFD.

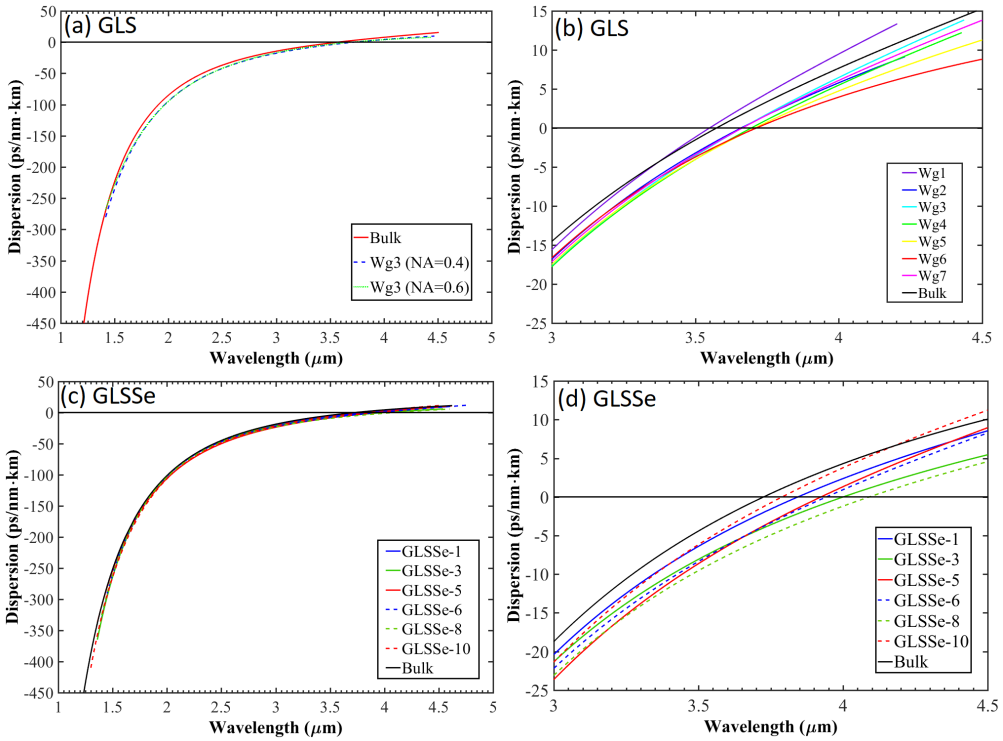

Fig. 4. GLS and GLSSe bulk and waveguide dispersion. a) Bulk and waveguide dispersion in GLS waveguides inscribed with different focusing optics and pulse energy. b) The intercept point showing the ZDW for a range of waveguides with increasing width. Bulk GLS ZDW is 3.61 µm with the waveguides being slightly higher in the range of 3.66-7.1 µm [16]. c) GLSSe dispersion in bulk and waveguide samples. d) The intercept point showing the ZDW for a range of waveguides with differing height and widths. Bulk GLSSe ZDW is seen to be 3.72 and waveguide ZDW is in the range of ~3.8-4.1 µm, again a slight increase.

Table 2. Inscription properties for GLS waveguides dispersion measurements[a]

Waveguide	Material	Width (µm)	Height (µm)	Pulse energy (nJ)	Speed (mm/s)	NA
Wg-1	GLS	3	18	110	12	0.6
Wg-2	GLS	5	18	110	12	0.6
$Wg\text{-}3_{0.4}$	GLS	7	18	64	12	0.4
Wg-3	GLS	7	18	110	12	0.6
Wg-4	GLS	9	18	110	12	0.6
Wg-5	GLS	11	18	110	12	0.6
Wg-6	GLS	13	18	110	12	0.6
Wg-7	GLS	15	18	110	12	0.6

[a]data is reproduced from Demetriou et al. [16].

Optical Materials EXPRESS

Measurements taken using the same experimental setup on the GLSSe waveguides used in this work show similar results. Results are presented for bulk GLSSe and waveguides inscribed using a range of parameters. In Fig. 4(c) we see, like for GLS, that the bulk and waveguide dispersion is similar. The ZDW for bulk GLSSe is 3.72 µm and in the waveguides it is slightly higher falling between 3.8 and 4.1 µm.

4. Waveguide supercontinuum generation

Waveguides were tested for SCG using a wavelength-tunable difference frequency generation (DFG) system (Spectra Physics), consisting of a Ti:Sapphire oscillator (MaiTai), a regenerative amplifier (Spitfire Ace), an optical parametric amplifier (TOPAS) and DFG extension module. The DFG system produces 100 fs pulses with energies of up to 20 µJ at 4 µm and tuneable from 2.4 to 11 µm. Horizontally polarized light was coupled into the waveguides using a 0.25 NA ZnSe objective (Innovation photonics, antireflection coated for 2 - 12 µm) and imaged using a 0.56 NA objective (Thorlabs, antireflection coated for 3-5 µm). The nearfield mode at the waveguide end facet was imaged onto a NEC uncooled microbolometer (IRV-T0831) for alignment and mode field diameter (MFD) determination. Once aligned, the signal was analyzed using a HORIBA iHR320 imaging monochromator equipped with a liquid nitrogen cooled 48-element MCT detector array and box-car integration system (Infrared Systems Development), as illustrated in Fig. 5. It was found that the larger waveguides exhibited broader SCG, which is attributed to the increased coupling efficiency between the input MFD and waveguide MFD and also the poor confinement of long-wavelength light in the smaller waveguides.

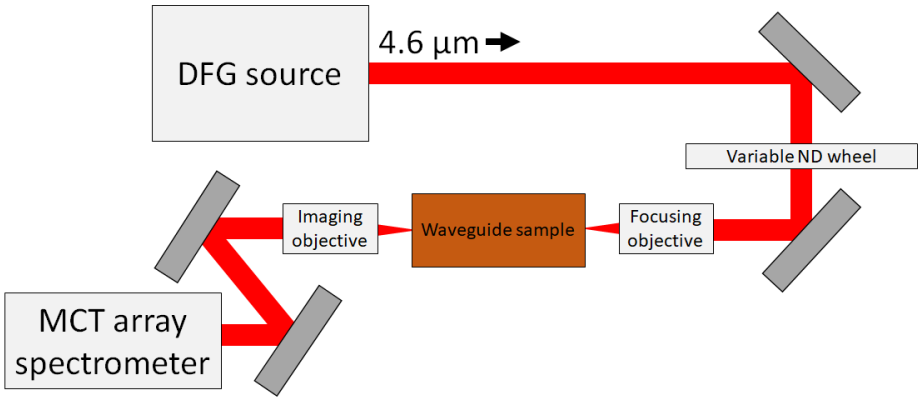

Fig. 5. Coupling setup for generating SC in GLS and GLSSe waveguide samples.

Waveguides were pumped at a range of wavelengths below and above the ZDW with the broadest output observed for pump pulses centered at 4.6 µm, in the anomalous dispersion regime, for this wavelength the MFD of waveguide GLSSe-1 was measured as 24.8 µm in the horizontal and 25.5 µm in the vertical direction. Typical SC spectra for one of the best performing waveguides (GLS-2) are shown in Fig. 6(a). Spectral broadening of high peak power ultrashort pulses with a high soliton number (calculated to be approximately 35 in this case for 900 nJ) in the anomalous dispersion regime close to the ZDW is dominated initially by strong self-phase modulation (SPM) followed by temporal compression, leading to soliton fission and the generation of dispersive waves (DWs) in the normal dispersion region. Further broadening of the long-wavelength edge is attributed to soliton self-frequency shifting due to the Raman effect (and possible soliton collisions at very high soliton numbers), which leads to a corresponding broadening towards shorter wavelengths of the short wavelength edge due to DWs being group-velocity matched to the red-shifting solitons. Such dynamics is consistent with the observed broadening in Fig. 6(a). At a pulse energy of 450 nJ we see a

Optical Materials EXPRESS

distinct DW peak at 2.15 µm whose corresponding soliton peak can be estimated from group-velocity matching. From the measured dispersion of the waveguide group-velocity matching with 2.15 µm corresponds to a soliton peak at around 5.39 µm, which is in reasonable agreement with the observed long-wavelength edge of the spectrum. When the pulse energy is increased to 900 nJ the shortest DW peak blue-shifts to around 1.93 µm as a consequence of enhanced soliton red-shifting, which from group-velocity matching calculations correspond to a soliton peak at 5.8 µm, similar to what is observed in the measurement.

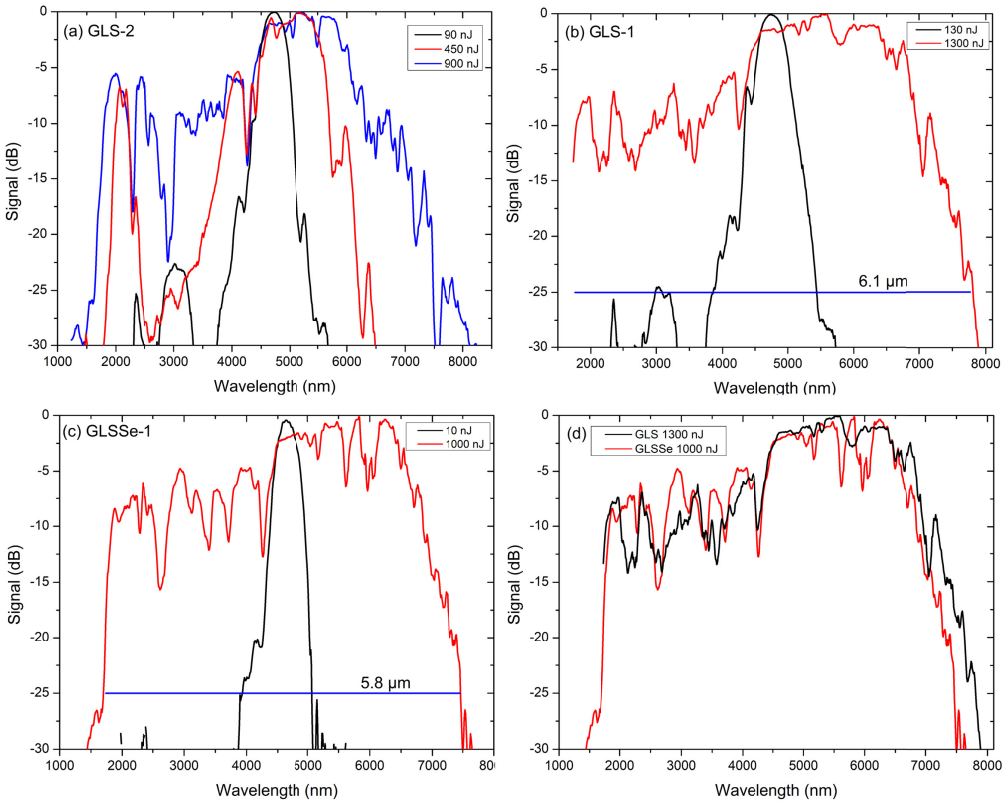

Fig. 6. SC spectra generated in GLS and GLSSe waveguides pumping at 4.6µm with 100fs pulses. (a) Typical evolution of the SC as the pulse energy is increased for 14 µm waveguide GLS-2, (b) 18 µm waveguide GLS-1 at high and low pulse energy, (c) 20 µm waveguide GLSSe-1 at high and low pulse energy and d) comparison between GLS-1 and GLSSe-1 from (b) and (c) showing the similarity between them.

In GLS we see SC spanning 6.1 µm from ~1.7-7.8 µm close to the long-wavelength transmission edge of the material. GLSSe waveguides yielded similar results with 5.8 µm of broadening and a similar cutoff. The peak power in the GLSSe waveguide was slightly lower than for GLS, 10MW compared to 13MW, with both samples operating close to their damage threshold, estimated to be ~1.5 µJ, 15 MW. The reduced power used in the GLSSe waveguide combined with operating closer to the sample zero-dispersion wavelength likely accounts for the slight decrease in broadening. These results suggest that whilst adding Se to the sample increases the long wavelength transmission edge we are limited by power in the waveguide. Investigating further sample composition, for increased damage resistance and nonlinearity may in future allow us to take advantage of the increased IR transmission. A comparison of GLS and GLSSe SC is shown in Fig. 6(d).

Optical Materials EXPRESS

5. Conclusions

We have demonstrated the suitability of ULI waveguides in GLS and GLSSe for mid-IR SCG. Pumping at 4.6 μm, in the anomalous regime, SCG in GLS spans almost the entirety of the transmission range of the glass with a width of 6.1 μm and long-wavelength edge of 8 μm. This result was achieved using 1.3 μJ energy pulses corresponding to a peak power of ~13 MW. To our knowledge this is the broadest and deepest IR SC demonstrated in a ULI waveguide to date. Experiments with low concentrations of Se added to GLS waveguides show similar broadening while the sample has increased long wavelength transmission. Optimising sample composition for increased transmission and damage resistance we predict that even broader SCG can be obtained in future investigations.

Funding

Innovation Fund Denmark (ShapeOCT, 4107-00011A); UK Engineering and Physical Sciences Research Council (CHAMP, EP/M015130/1; IDC Opt. Phot. Tech., EP/G037523/1).

Acknowledgments

The data sets generated during and/or analysed during the current study are available from the corresponding author on reasonable request.

References

1. R. R. Thomson, A. K. Kar, and J. Allington-Smith, "Ultrafast laser inscription: an enabling technology for astrophotonics," Opt. Express **17**(3), 1963–1969 (2009).
2. B. J. Eggleton, B. Luther-Davies, and K. Richardson, "Chalcogenide photonics," Nat. Photonics **5**(3), 141–148 (2011).
3. D. W. Hewak, "Chalcogenide glasses for photonics device applications," in *Photonic glasses and glass-ceramics (Ed. GS Murugan)* (Research Signpost, 2010).
4. C. R. Petersen, U. Moller, I. Kubat, B. B. Zhou, S. Dupont, J. Ramsay, T. Benson, S. Sujecki, N. Abdel-Moneim, Z. Q. Tang, D. Furniss, A. Seddon, and O. Bang, "Mid-infrared supercontinuum covering the 1.4-13.3 mu m molecular fingerprint region using ultra-high NA chalcogenide step-index fibre," Nat. Photonics **8**(11), 830–834 (2014).
5. A. Ravagli, C. Craig, G. A. Alzaidy, P. Bastock, and D. W. Hewak, "Optical, Thermal, and Mechanical Characterization of Ga_2 Se_3 -Added GLS Glass," Adv. Mater. **29**(27), 1606329 (2017).
6. A. Ravagli, C. Craig, J. Lincoln, and D. W. Hewak, "Ga-La-S-Se glass for visible and thermal imaging," Adv. Opt. Technol. **6**, 131–136 (2017).
7. J. McCarthy, H. Bookey, S. Beecher, R. Lamb, I. Elder, and A. K. Kar, "Spectrally tailored mid-infrared super-continuum generation in a buried waveguide spanning 1750 nm to 5000 nm for atmospheric transmission," Appl. Phys. Lett. **103**(15), 151103 (2013).
8. N. D. Psaila, R. R. Thomson, H. T. Bookey, S. Shen, N. Chiodo, R. Osellame, G. Cerullo, A. Jha, and A. K. Kar, "Supercontinuum generation in an ultrafast laser inscribed chalcogenide glass waveguide," Opt. Express **15**(24), 15776–15781 (2007).
9. J. M. Morris, M. D. Mackenzie, C. R. Petersen, G. Demetriou, A. K. Kar, O. Bang, and H. T. Bookey, "Ge22As20Se58 glass ultrafast laser inscribed waveguides for mid-IR integrated optics," Opt. Mater. Express **8**(4), 1001–1011 (2018).
10. D. Choudhury, J. R. Macdonald, and A. K. Kar, "Ultrafast laser inscription: perspectives on future integrated applications," Laser Photonics Rev. **8**(6), 827–846 (2014).
11. J. Morris, N. K. Stevenson, H. T. Bookey, A. K. Kar, C. T. A. Brown, J. M. Hopkins, M. D. Dawson, and A. A. Lagatsky, "1.9 μm waveguide laser fabricated by ultrafast laser inscription in Tm:Lu_2O_3 ceramic," Opt. Express **25**(13), 14910–14917 (2017).
12. A. A. S. Ph. Bado, and Mark Dugan, "Manufacturing of high quality integrated optical components by laser direct-write " Journal of Laser Applications (2003).
13. Y. Yu, X. Gai, P. Ma, K. Vu, Z. Yang, R. Wang, D.-Y. Choi, S. Madden, and B. Luther-Davies, "Experimental demonstration of linearly polarized 2-10 μm supercontinuum generation in a chalcogenide rib waveguide," Opt. Lett. **41**(5), 958–961 (2016).
14. H. T. Bookey, R. R. Thomson, N. D. Psaila, A. K. Kar, N. Chiodo, R. Osellame, and G. Cerullo, "Femtosecond laser inscription of low insertion loss waveguides in Z-cut lithium niobate," IEEE Photonics Technol. Lett. **19**(12), 892–894 (2007).
15. P. Hlubina, D. Ciprian, and M. Kadulova, "Measurement of chromatic dispersion of polarization modes in optical fibres using white-light spectral interferometry," Meas. Sci. Technol. **21**(4), 7 (2010).

Optical Materials EXPRESS

16. G. Demetriou, J. P. Bérubé, R. Vallée, Y. Messaddeq, C. R. Petersen, D. Jain, O. Bang, C. Craig, D. W. Hewak, and A. K. Kar, "Refractive index and dispersion control of ultrafast laser inscribed waveguides in gallium lanthanum sulphide for near and mid-infrared applications," Opt. Express **24**(6), 6350–6358 (2016).
17. I. Kubat, C. S. Agger, U. Møller, A. B. Seddon, Z. Tang, S. Sujecki, T. M. Benson, D. Furniss, S. Lamrini, K. Scholle, P. Fuhrberg, B. Napier, M. Farries, J. Ward, P. M. Moselund, and O. Bang, "Mid-infrared supercontinuum generation to 12.5μm in large NA chalcogenide step-index fibres pumped at 4.5μm," Opt. Express **22**(16), 19169–19182 (2014).